ICIC Express Letters
Part B: Applications
Volume **7**, Number **9**, September **2016**
ICIC International ©2016 ISSN 2185-2766
pp. 1871–1877

INFLUENCE OF OBSTACLE LAYOUT ON THE EXPLOSION OVERPRESSURE WITHIN THE UPPER DECK OF AN OFFSHORE OIL PLATFORM

Pengcheng Wang

Marine Engineering College
Dalian Maritime University
No. 1, Linghai Road, Dalian 116026, P. R. China
wpc6688@163.com; wangpch2@cnooc.com.cn

Received February 2016; accepted May 2016

Abstract. *The influence of obstacle layout on the explosion overpressure within the upper deck of an offshore oil platform is presented in this paper. Obstacles of different shapes and volumes are placed within the upper deck of an offshore platform. Their effects on the explosion overpressure within the upper deck are numerically studied by the AutoReaGas software. The results show that the obstacle can greatly increase the peak explosion pressure in the upper deck. Also, the cuboid obstacle is more effective on increasing the overpressure than the cylindrical obstacle. For the obstacles with the same shape, the peak overpressure increases with the increase in the volume. The research results show that, comparing with no obstacles, the peak overpressure increases obviously in the situations of obstacles. In addition, cuboid obstacles make more effects on improving the peak overpressure than cylindrical obstacles; however, the advantages decrease when the volume increases. In contrast, the peak overpressure increases with volume rising in the same shape of obstacles. These results can provide reference to the reasonable layout of equipment on the offshore oil platform and have a beneficial effect on natural explosion in open space.*
Keywords: Natural gas explosion, Peak overpressure, Obstacle, Offshore oil platform

1. **Introduction.** Gas explosion is a serious accident for many industries, including chemical, coal mining and offshore oil exploitation. It may cause great damage to the equipment, people and even bring unacceptable pollution to the environment [1]. For example, on April 21, 2010, the Deepwater Horizon oil platform, located in the Mississippi Canyon about 40 miles off the Louisiana coast, suffered a catastrophic explosion and sank a day-and-a-half later. Despite the safety management measures getting strict in recent years, there are still many gas explosion accidents. Meanwhile, it has been proved that the layout of obstacles can affect the overpressure distribution when gas explosion occurs [2].

In recent years, the numerical simulations of gas explosion have been extensively investigated and a number of meaning results have been obtained. Jiang et al. [3,4] use numerical simulation to get the safe distance of gas deflagration in the coal mine. Zhu et al. [5] investigate the effect of blast wave oscillations generated by overpressure in the premixed methane/air explosion. In addition, the influence of obstacles, especially multiple obstacles in gas explosion has been well studied [6,7]. Previous work shows that the obstacles play an important role in the gas explosion and the position, shape, quantity and volume have great influence on the overpressure in the gas explosion. The damage caused by the explosion may be minimized by proper layout of the production equipment and explosion-proof walls. However, the previous research mainly focuses on the obstacles of planar geometry structure, such as the repetition barrier, the barrier ring, and the sector plate. In fact, most of the equipment can be simplified as many cylindrical obstacles and cuboid obstacles in the calculation of gas explosion, so it is necessary to study the three dimensional obstacles according to the actual needs. In this paper, models of explosion are built with three dimensional obstacles so as to simulate the explosion within the upper deck of offshore oil platform by AutoReaGas which is chosen for the wide use in studies of explosion [6-8]. By analyzing these results qualitatively and quantitatively, the proper layout of obstacles can be obtained and be used for the real industrial production.

2. Basic Equations and Numerical Models.

2.1. **Basic equation.** The software of AutoReaGas has been verified, and the simulative prediction and test results are better in the famous BFETS test. A large body of experimental data on turbulent flame propagation is correlated by Bray [9], the relationship between the speed of turbulent, turbulent parameters and mixture properties.

$$\boldsymbol{S}_t = 1.8\boldsymbol{u}'^{0.412}.\boldsymbol{L}_t^{0.196}.\boldsymbol{S}_l^{0.784}.\boldsymbol{\nu}^{-0.196} \tag{1}$$

where $\boldsymbol{S}_t$ is the turbulent burning speed, $\boldsymbol{u}'$ is the turbulent intensity, $\boldsymbol{L}_t$ is the turbulence characteristic length scale (integral scale), $\boldsymbol{S}_l$ is laminar burning velocity flammable mixture and $\boldsymbol{\nu}$ is the kinematic viscosity of the unburned flammable mixture. The effect of temperature, pressure and front wrinkling of flame on the laminar burning velocity are described by a second adjustable parameter $\boldsymbol{F}_s$ which relates $\boldsymbol{S}_b$ to the flame radius $\boldsymbol{r}_m$ and to the theoretical laminar flame speed as follows [10]:

$$\boldsymbol{S}_b = \boldsymbol{S}_1(1 + \boldsymbol{F}_s\boldsymbol{r}_m) \tag{2}$$

The constants used for simulations of premixed gas explosions are given in Table 1.

Table 1. The set of constants used for simulations

Variable	*Value*
Gamma	*1.25*
Methane composition (%volume)	*9.5%*
Heat of combustion	2.751×10^6 *J/kg*
Lower flammable limit (%mass)	*2.82%*
Upper flammable limit (%mass)	*8.87%*
Burning velocity	*0.45m/s*
Flame speed factor	*0.15*
Viscosity	2.5×10^{-5} Ns/m^2
Turbulent combustion modelling constant	*70*
Temperature	*300K*
Atmospheric pressure	1.025×10^5 *Pa*

2.2. **Numerical models.** The upper deck of offshore oil platform has been constructed and obstacles of different shapes have been sited on four circles. These obstacles are uniformly distributed in each circle and the radii of circles are 5m, 10m, 15m and 20m, and the center of these circles is sited in the position of ignition source. The quantities of obstacles are 8, 16, 24 and 32, which are sited on circles separately and averagely. Figure 1(a) shows the distribution of cylindrical obstacles. And Figure 1(b) shows the distribution of cuboid obstacles. The computational domain of offshore oil platform model in upper deck is 50m × 50m × 5m and the ignition source is sited in the center of the domain and the coordinate in Cartier coordinate system is (0,0,0).

Around the perimeter of the model and the top is sited as "open" boundary, the bottom surface is sited as "solid" boundary. The coordinates of gauged points are: gauge1 (0,0,2.25), gauge2 (0,0,7.25), gauge3 (0,0,12.25), gauge4 (0,0,17.25), and gauge5 (0,0,22.25). These gauged points and boundaries are shown in Figure 1.

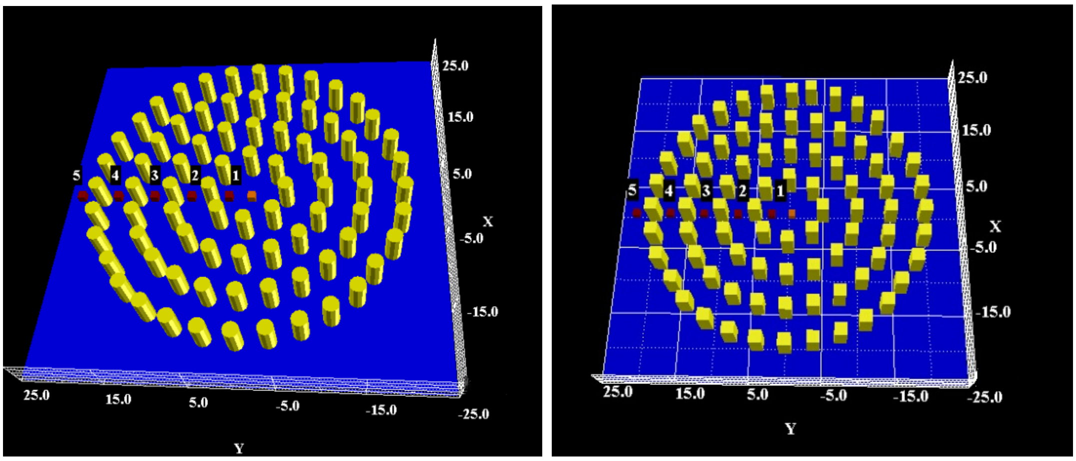

(a) (b)

Figure 1. The positions of obstacles: (a) cylindrical obstacles, five gauged points and ignition source; (b) cuboid obstacles, five gauged points and ignition source

Table 2. Working conditions of simulation

Working condition	R=10m/H=5m			R=10m/H=5m			R=15m/H=5m			R=20m/H=5m		
	Q	S	V (m^3)	Q	S	V (m^3)	Q	S	V (m^3)	Q	S	V (m^3)
UPAO	*0*	*NA*	*0*	*0*	*NA*	*0*	*0*	*NA*	*0*	*0*	*NA*	*0*
$UPCY_4$	*8*	*Cy*	*3.9*	*16*	*Cy*	*3.9*	*24*	*Cy*	*Cy*	*32*	*Cy*	*3.9*
$UPCU_4$	*8*	*Cu*	*3.9*	*16*	*Cu*	*3.9*	*24*	*Cu*	*Cu*	*32*	*Cu*	*3.9*
$UPCY_8$	*8*	*Cy*	*15.9*	*16*	*Cy*	*15.9*	*24*	*Cy*	*Cy*	*32*	*Cy*	*15.9*
$UPCU_8$	*8*	*Cu*	*15.9*	*16*	*Cu*	*15.9*	*24*	*Cu*	*Cu*	*32*	*Cu*	*15.9*
$UPCY_{12}$	*8*	*Cy*	*34.9*	*16*	*Cy*	*34.9*	*24*	*Cy*	*Cy*	*32*	*Cy*	*34.9*
$UPCU_{12}$	*8*	*Cu*	*34.9*	*16*	*Cu*	*34.9*	*24*	*Cu*	*Cu*	*32*	*Cu*	*34.9*
Notes: "Cy" represents the cylindrical obstacle, "Cu" represents the cuboid obstacle, "V" represents the volume of obstacle, "H" represents the height of obstacle, "R" represents the distance between the ignition source and the center of obstacle, "Q" represents the quantity of obstacle, and "S" represents the shape of obstacle.												

3. **Numerical Simulation.** In this section, we give the working conditions for simulation and carry out numerical simulation to get the relative results.

3.1. **Working conditions of simulation.** In order to find the influence by different obstacles, seven working conditions of simulation are sited in Table 2.

3.2. **Simulative result without any obstacle.** In order to compare the influence of overpressure with obstructed environment, the simulation result without any obstacle is shown in Figure 2.

3.3. **Simulative results with obstacles.** Six simulative results with different shapes and volumes are generated and these results are shown in Figures 3-5.

4. **Discussion.** First, it is obvious that the obstacles greatly increase the peak pressure compared with the condition without any obstacle. Furthermore, in order to find the rules of peak overpressure influenced by different shapes of obstacles in the upper deck of oil offshore platform, the simulative results of peak overpressure are compared in Figure 6. It

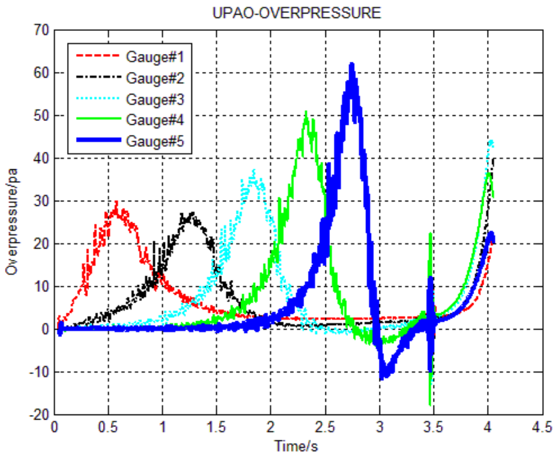

FIGURE 2. Overpressure result without any obstacle

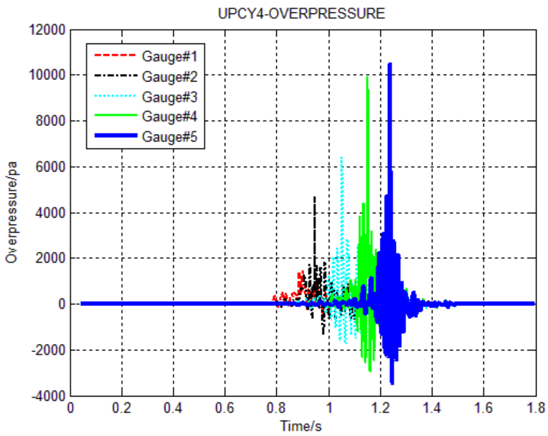

(a)

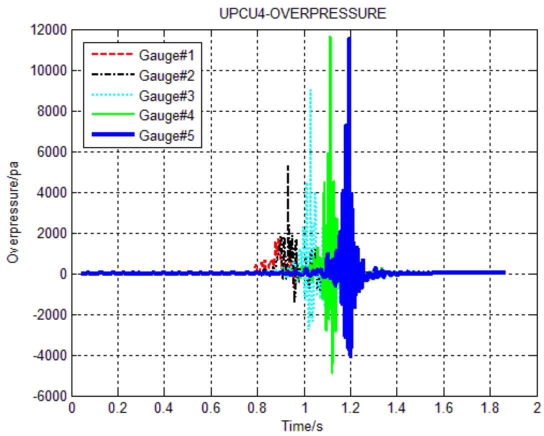

(b)

FIGURE 3. Overpressure with 3.9m^3 of each obstacle: (a) cylindrical; (b) cuboid

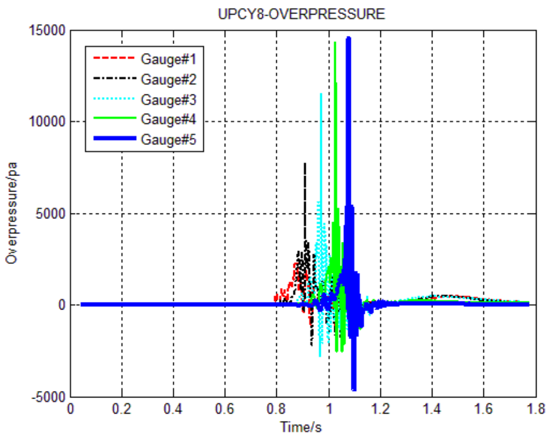

(a)

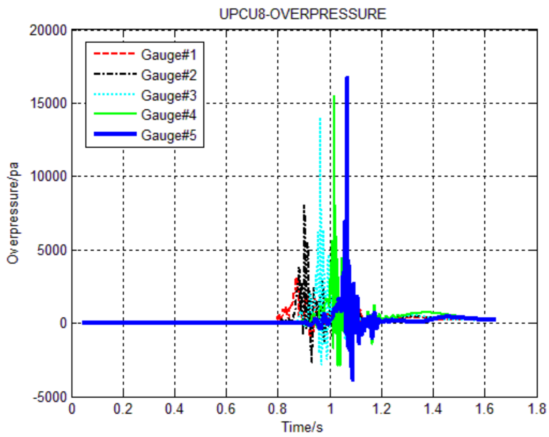

(b)

FIGURE 4. Overpressure with 15.9m^3 of each obstacle: (a) cylindrical; (b) cuboid

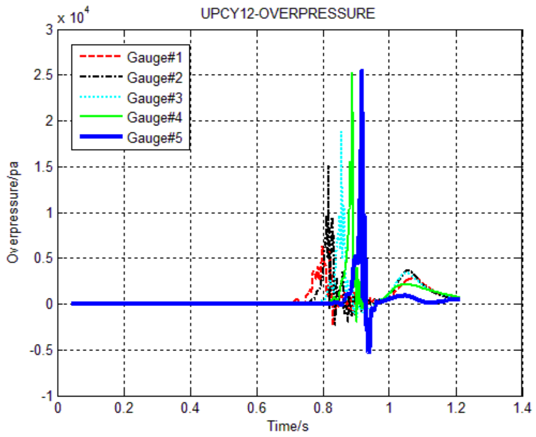

(a)

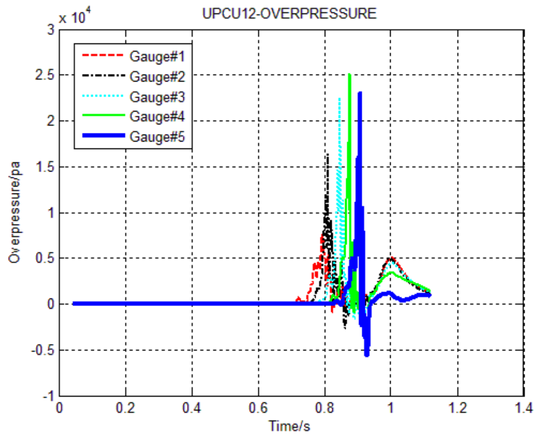

(b)

FIGURE 5. Overpressure with 34.9m^3 of each obstacle: (a) cylindrical; (b) cuboid

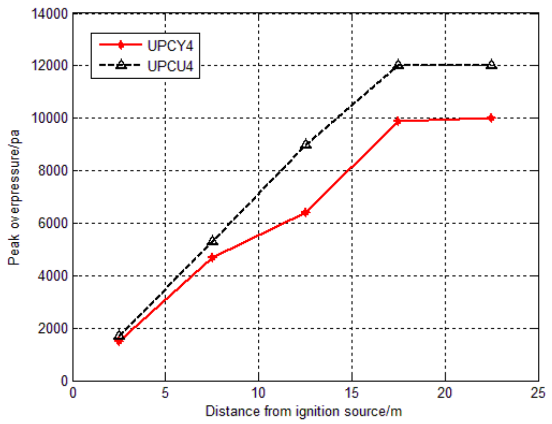

(a)

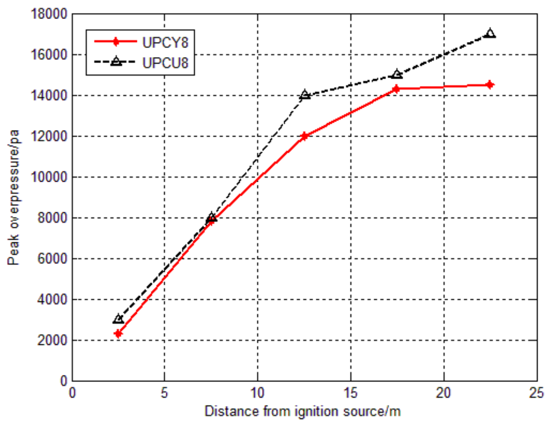

(b)

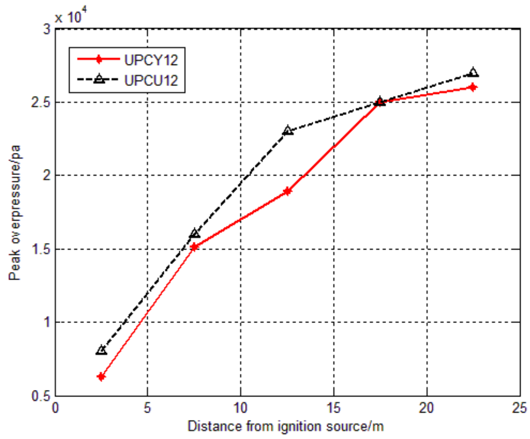

(c)

FIGURE 6. The relationship between peak overpressure and distance from ignition source to gauged points, while the obstacles have the same volume but different shapes: (a) each cylindrical and cuboid obstacle volume being 3.9m^3; (b) each cylindrical and cuboid obstacle volume being 15.9m^3; (c) each cylindrical and cuboid obstacle volume being 34.9m^3

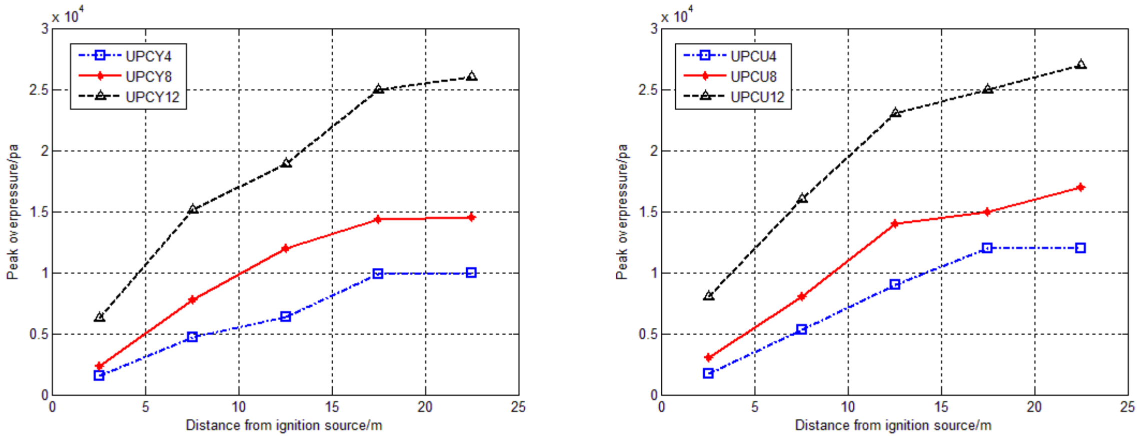

(a) (b)

Figure 7. The relationship between peak overpressure and distance from ignition source to gauged points, while the obstacles have the same shape but different volumes: (a) the cylindrical obstacles with different volume of each, $UPCY_4 = 3.9m^3$, $UPCY_8 = 15.9m^3$, $UPCY_{12} = 34.9m^3$; (b) the cuboid obstacles with different volume of each, $UPCU_4 = 3.9m^3$, $UPCU_8 = 15.9m^3$, $UPCU_{12} = 34.9m^3$

compares cylindrical obstacles with cuboid obstacles in three volumetric situations, and the volume of each obstacle is the same in the same volumetric situations. The rules are found that the peak overpressure increases quickly along the distance from the center to the edge, if these two shapes of obstacles are sited in the natural gas explosion models. In addition, the cuboid obstacles make a huger effect on increasing the peak overpressure than cylindrical obstacles when they are in the same volumetric situations. Then, the simulative results of peak overpressure have been compared in Figure 7 which have the same shape but different volumes. We can see that cuboid obstacles and cylindrical obstacles contribute to the role of the peak overpressure value with the same trend along the distance from ignition source, and the peak overpressure increases with the volume increasing obviously.

5. **Conclusions.** This work presents a study on the influence of overpressure on natural gas explosion shock wave under the obstructed situations of different shapes and volumes. In the whole simulation of explosion, the obstacles increase the peak overpressure obviously by comparing with the situations without any obstacle. The maximum of peak overpressure appears near the edge of offshore oil platform and the minimum appears near the center. Different shapes and volumes give rise to obvious differences about peak overpressure caused by natural gas explosion shock wave. On the one hand, comparing to cylindrical obstacles, the cuboid obstacles have obviously positive effect on improving the peak overpressure. However, the gap decreases when the volume increases. On the other hand, the larger volume of obstacles can cause more destructive explosion shock wave and the higher peak overpressure. For the requirement of technical design and loss control, the volume of obstacles should be minimized as much as possible and cylindrical obstacle shapes should be used instead of cuboid obstacles if possible so as to reduce the potential risks. However, the rules of explosion caused by combinative obstacles and the balance point between limited space and the volume of obstacles should be studied in the future.

REFERENCES

[1] B. H. Hjertager, T. Solberg and K. O. Nymoen, Computer modeling of gas explosion propagation in offshore modules, *Journal of Loss Prevention in the Process Industries*, no.5, pp.165-174, 1992.
[2] S. S. Ibrahim and A. R. Masri, The effects of obstructions on overpressure resulting from premixed flame deflagration, *Journal of Loss Prevention in the Process Industries*, vol.14, no.3, pp.213-221, 2001.
[3] B. Y. Jiang, B. Q. Lin, S. L. Shi et al., A numerical simulation of the influence initial temperature has on the propagation characteristics of and safe distance from a gas explosion, *International Journal of Mining Science and Technology*, no.22, pp.307-310, 2012.
[4] B. Y. Jiang, B. Q. Lin, S. L. Shi et al., Numerical simulation on the influences of initial temperature and initial pressure on attenuation characteristics and safety distance of gas explosion, *Combustion Science and Technology*, no.184, pp.135-150, 2012.
[5] C. J. Zhu, B. Q. Lin, B. Y. Jiang et al., Numerical simulation of blast wave oscillation effects on a premixed methane/air explosion in closed-end ducts, *Journal of Loss Prevention in the Process Industries*, no.26, pp.851-861, 2013.
[6] D. J. Park, Y. S. Lee and R. G. Anthony, Prediction for vented explosions in chambers with multiple obstacles, *Journal of Hazardous Materials*, no.155, pp.183-192, 2008.
[7] A. R. Masri, S. S. Ibrahim, N. Nehzat et al., Experimental study of premixed flame propagation over various solid obstructions, *Experimental Thermal and Fluid Science*, no.21, pp.109-116, 2000.
[8] L. Pang, T. Wang, Q. Zhang et al., Nonlinear distribution characteristics of flame regions from methane – Air explosions in coal tunnels, *Process Safety and Environmental Protection*, no.92, pp.193-198, 2014.
[9] K. N. C. Bray, Studies of the turbulent burning velocity, *Proc. of the Royal Society of London*, vol.431, pp.315-325, 1990.
[10] E. Salzano, F. S. Marra, G. Russo et al., Numerical simulation of turbulent gas flames in tubes, *Journal of Hazardous Material*, vol.95, pp.233-247, 2002.